NATURAL FREQUENCY RESPONSE OF RIGID, CELLULAR SUPPORTED COMPOSITE PLATES

C. B. York
Department of Aerospace Engineering,
University of Glasgow,
James Watt Building,
Glasgow G12 8QQ
Scotland, UK.

Keywords: *Natural Frequency, Eigenvalue, Hexagonal, Skew, Specially Orthotropic*

Abstract

An assessment of the natural frequency response for thin, laminated plate arrays is presented for various optimal buckling-strength to weight ratio planform configurations. Comparison is made between isotropic (aluminium) and composite material, in which the laminate stacking sequences have specially orthotropic properties, allowing the use of closed form solutions for the assessment of standard rectangular planform cases. The study also considers the effect on the natural frequency of in-plane loading, below the initial buckling load.

1 General Introduction

The natural frequency response of rectangular plates has been very extensively studied for a wide range of boundary conditions. Much of the earliest work dealing with natural frequency predictions in plate structures is described in the monographs of Timoshenko [1], Meirovitch [2] and Chen [3] with shorter reviews continuing alongside the associated technical advances in this area. Over the last few decades the number of studies dealing with skew plate structures [4]-[7] has also seen a large increase. By contrast, fewer studies have considered the response of plate structures with other plan-form geometries. Exceptions [8] include an experimental investigation [9] of the natural frequency of a regular hexagonal plate, including mode shape prediction using the finite element method.

In most studies of natural frequency response, the adopted boundary conditions have been clamped, simply supported, free or combinations of these. Although these boundary conditions are useful in providing upper- or lower-bound solutions to a more general problem, they often lead to a loss of economy and accuracy in design because they do not permit the benefits of structural continuity to be included appropriately in the design process. In a real structure there is usually some form of continuity between adjacent panels and/or other structural elements, which offers both bending and torsional stiffness to the plate edges. However, few results are available which demonstrate the effects of plate continuity [10], [11].

A new stiffness matrix method formulation [12] is used to obtain the natural frequency predictions. This method is based on exact flat plate theory and assumes that the plate is continuous over supports, whereby the response of one cell of the plate array influences the response in adjacent cells. The approach is similar to that for the equivalent buckling problem [13], which has been applied to rectangular [14] and skew plate [15] assemblies and more recently to arrays of regular hexagonal plates [16]. These more complex support

geometries have been shown to provide significant buckling strength increases coupled with a reduction in the perimeter length of the supporting stiffener (hence structural weight), compared with traditional stiffener arrangements forming rectangular or square cells. Panels with these particular attributes are of potentially great benefit in weight critical structures. The keel panels of the projecting aft-fuselage section, shown in **Fig. 1**, constitute weight critical components that are subject to significant in-plane loads due to the combined action of the vertical and horizontal tails. Structural components in this part of the aircraft are also subject to a broad spectrum of excitation frequencies.

Fig. 1 – Aft fuselage section, supporting the vertical and horizontal tails on the JSF.

In this paper, therefore, the natural frequency response of cellular supported plate arrays is investigated, see **Fig. 2**, which complement previous buckling studies [16] on these types of stiffened panel configuration.

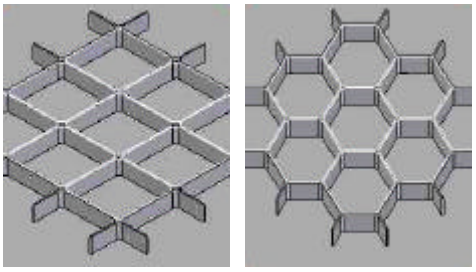

Fig. 2 – Comparison of square (traditional) and hexagonal stiffener patterns forming equal area cells.

The results are presented as design curves to highlight parametric interaction and in tabular format for benchmarking purposes, which include the comparison of frequency responses for isotropic (aluminium) and equal mass composite plates with specially orthotropic properties. A selection of the results is validated against a finite element solution [17] and against standard results in the literature for isolated plates with simply supported and clamped boundary conditions. Results are also presented for a selection of in-plane loaded panels; below the initial buckling load.

Mathematical Approach

Although buckling and vibration problems are generally treated separately from a physical point of view, computationally they may be regarded as the same. Lurie [18] and Wittrick and Williams [19] showed that for plates with the same in-plane elastic moduli and density, the live load system of the buckling problem is related to the natural frequency by the simple formula:

$$(\sigma_L)_m = 4\rho\lambda^2 n^2_m \qquad (1)$$

Where $(\sigma_L)_m$ is the m^{th} buckling stress and n_m is the m^{th} natural frequency.

This formula is used as a check on all the square panel results, including composite laminate results, where $(\sigma_L)_m$ is derived from the closed form buckling solution.

$$\sigma_L = \frac{\pi^2}{b}\left[D_{11}\left(\frac{m}{a}\right) + 2\left(D_{12} + 2D_{66}\right)\left(\frac{n}{b}\right)^2 + D_{22}\left(\frac{n}{b}\right)^4\left(\frac{a}{m}\right)^2 \right] \quad (2)$$

in which the D_{ij} are plate flexural stiffnesses, and *m* and *n* are integer half-waves over the plate length *a* and *b*, respectively.

The remainder of this section gives a brief summary of the theory used for calculating the natural frequencies of undamped free vibrations for an infinitely wide panel in which only one repeating bay of the structure is considered [12].

Fig. 3(a) shows a component plate of width b, with the basic longitudinally invariant in-plane forces to which it is subjected. In a vibration problem, these forces are regarded as defining the datum state (dead load) of the structure about which small vibrations occur. In the buckling problem, these forces give rise to instability. They consist of N_L, N_T and N_S per unit length, corresponding to uniform longitudinally and transverse compressive force and a uniform shear flow, respectively.

The plate deflection is assumed to vary sinusoidally in the longitudinal, x, direction with half-wavelength, λ, and with displacement amplitudes u, v,and w relating to the axes x, y, z, see **Fig. 3**(b). For isotropic or orthotropic plates and $N_S = 0$, the nodal lines or lines of zero displacement of the deflection pattern are perpendicular to the longitudinal direction. The results are then consistent with transverse simply supported end conditions of each plate of the assembly and so exact results are obtained for such end conditions if λ is taken as $\lambda_j = a/j$, where j = 1, 2, 3, ….

Displacements at nodes or junctions between the longitudinal plates are given by the real part of

$$\mathbf{D}'_j \exp(i\pi x/\lambda_j).\cos 2\pi nt \quad (3)$$

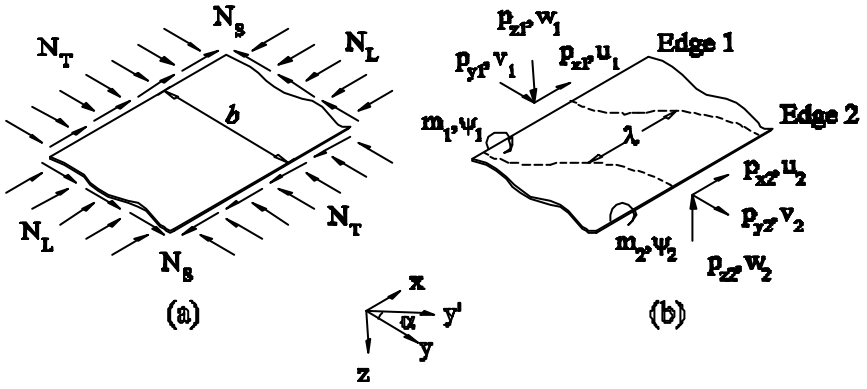

Fig. 3 - An infinitely long component plate: (a) of width b and illustrating the loading system; (b) showing skewed nodal lines with half-wavelength ? caused by perturbation force (denoted by p and m) and displacement amplitudes shown at the longitudinal edges of the plate.

where $i = \sqrt{-1}$, n and t are the frequency and time (n is taken to be zero in a buckling problem), x is the longitudinal co-ordinate and $\mathbf{D}'_j$ contains the four complex displacement amplitudes for each of the N node which correspond, in order, to the ψ, w, v and u. The resulting $4N \times 4N$ stiffness matrix $\mathbf{K}_j$ corresponds to $\mathbf{D}_j$, where $\mathbf{D}_j$ is the vector obtained by multiplying all longitudinal displacements in $\mathbf{D}'_j$ by i, to account for u being 90° out of phase with v, w and ψ.

$\mathbf{K}_j$ is a dynamic stiffness matrix which is hermitian and becomes real and symmetric if no plates are anisotropic [or subject to a static shear load]. It was derived explicitly by solving the appropriate differential equations and has uncoupled anisotropic out-of-plane (i.e. flexural) and orthotropic in-plane properties, i.e. $A_{16} = A_{26} = B_{ij} = 0$.

The natural frequencies (or critical loads) are the eigenvalues corresponding to $\mathbf{K}_j\mathbf{D}_j = \mathbf{0}$. Because $\mathbf{K}_j$ is a transcendental function of λ_j and the frequency (or load factor), a general algorithm is employed, based essentially on an extension to the Sturm sequence procedure for the linear eigenvalue problem [20], to ensure that no natural frequencies are missed for exact (as opposed to, for example, finite element) stiffness matrix analyses of undamped free vibration of linear elastic structures.

The stiffness matrices, $\mathbf{K}$, for appropriate values of λ are coupled by the method of Lagrangian Multipliers. This permits the plate assembly to be attached to any combination of arbitrary located point supports, by producing constraints in bay 1 of the infinitely long structural system which automatically repeats at bay long intervals a.

The mode of vibration is assumed to repeat over M bays, i.e. over a length $L = Ma$. All required modes could be obtained by simultaneously satisfying these equations,

$$a\mathbf{K}_m\mathbf{D}_m + \mathbf{e}_m{}^H g_n = \mathbf{0} \qquad (4)$$

$$\Sigma\mathbf{e}_m\mathbf{D}_m = \mathbf{0}$$

$$(m = n + qM;\ q = 0, \pm1, \pm2, \ldots)$$

for, in turn, each of the integers n given by

$$-M'' \le n \le M' \qquad (5)$$

where M″ and M′ are, respectively, the integer parts of (M-1)/2 and M/2.

In Eqns (4), the number of q values used governs the accuracy obtained. g_n and $\mathbf{e}_m$ are the Lagrangian Multipliers vectors and constraint matrices respectively while $\mathbf{K}_m$ are the stiffness matrices.

The constraint matrix,

$$\mathbf{e}_m = e'\exp(2i\pi mx/L) \qquad (6)$$

has as many rows as there are constraints in a single bay and elements of e′ are either 0 or 1.

The solution contains all modes with wavelength L, L/2, L/3, etc. Hence, because $\lambda_m = L/2m$ and $L = Ma$, the values of m previously defined in Eqns (4) gives:

$$\lambda_m = a/\{(2n/M) + 2q\} \qquad (7)$$

$$q = 0, \pm1, \pm2, \ldots$$

From Eqn. (7), the λ_m are a function of M/*n* and not of M and *n* independently. Therefore, considering only combinations of M and *n* which share the same value of M/*n* leads to computational savings. It is therefore practical to express the resulting relationships in terms of the single parameter $x = 2n/M$, so that Eqn. (7) can be written as

$$\lambda_m = \frac{a}{x + 2q} \qquad (8)$$

$q = 0, \pm 1, \pm 2, \ldots$

Higher accuracy is achieved in the analysis by increasing both q_{max}, the maximum value of q and the number of x terms in the range $0 \le x \le 1$.

Repetitive analysis

Many plate assemblies exhibit repetitive cross-sections, which can be analysed by suitable recurrence equations, based on an infinite width assumption. For skew or hexagonal plate assemblies, constraints must be included in these recurrence equations such that the compatibility of the supports is maintained in adjacent bays. For the hexagonal planform geometry, shown in **Fig. 4**, neither (a) the uni-axial nor (b) bi-axial cases possess the necessary geometric features of the hexagonal array. However, the introduction of a constant longitudinal shift (χ) to support locations at the start of each transversely adjacent portion provides the desired effect, see **Fig. 4**(c).

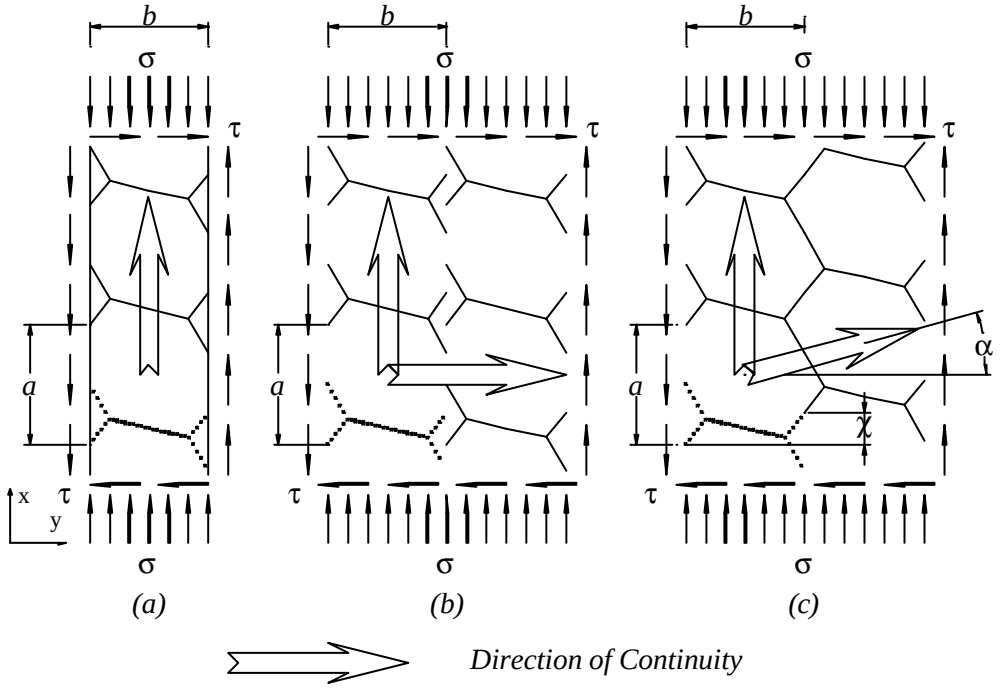

Fig. 4 - Support conditions for hexagonal plate with: (a) uni-axial continuity - boundary conditions enforced by Lagrangian multiplier method, i.e. discrete point constraints repeat at bay length intervals, *a*; (b) bi-axial (transverse) continuity - enforced by recurrence equation, i.e. mode repeats at bay width intervals, *b* and (c) Skew-transverse continuity – as (b) with phase shift c in the adjacent bay.

The fundamental equations for a repeating portion or the hexagonal array become:

$$a\mathbf{K}_{m0}\mathbf{D}_{m0} + \mathbf{e}_{m0}{}^{H}g_{n0} = \mathbf{0} \quad (9)$$

$$\Sigma\mathbf{e}_{m0}\mathbf{D}_{m0} = \mathbf{0}$$

$$(m = n + qM;\ q = 0, \pm1, \pm2, \ldots)$$

where

$$\mathbf{K}_{m0} = \mathbf{K}_{m11} + \mathbf{K}_{m12}{}^{H}\exp\{-i(\phi - 2\pi m\chi/Ma)\} + \mathbf{K}_{m12}\exp\{i(\phi - 2\pi m\chi/Ma)\} \quad (10)$$

Equations must be solved for the same values of ξ as for plate assemblies that are not transversely repetitive. However, now suitable values of ϕ must be used for each combination.

When $\chi = 0$, Eqns (9) and (10) reduce to the previous form for transversely repetitive panels of rectangular plan-form [21].

$$\mathbf{K}_{m0} = \mathbf{K}_{m11} + \mathbf{K}_{m12}{}^{H}\exp(-i\phi) + \mathbf{K}_{m12}\exp(i\phi) \quad (11)$$

and the values of ϕ describes the mode which repeat across twice the width of the assembly, so that, if P is the number of repeating portions of width b within the assembly,

$$\phi = \pi g/P \quad (12)$$

$$g = -(P - 1),\ldots,-1,0,1,\ldots,P.$$

and the transverse half-wavelength λ_T is

$$\lambda_T = Pb/g = \pi b/\phi \quad (13)$$

Because $\alpha \neq 0°$ is now the general case, $\chi \neq 0$ in **Fig. 4**(c) and so the mode repeats over twice the width Pb of the assembly except that it is now moved along the assembly by 2χ, such that it is skewed by the angle α, where $\chi = b.\tan\alpha$. Hence λ_T is the component, perpendicular to the longitudinal axis, of a half-wavelength that is skewed by the angle, α.

Geometric details and Computer modelling

Fig. 5 defines the plan-form geometry for seven array configurations considered. The figure is divided into four columns containing the skew arrays $\alpha = 0°$, $\pm15°$, $\pm30°$ and $\pm45°$ forming a template onto which the equivalent hexagonal array is mapped. Mapping involves the superposition of the geometric centre points of each cell of the hexagonal plate array with those of the skew array template. All geometries are defined by a single aspect ratio $a = b = 1.0$ applied to the skew array, measured along the x- and y-axes respectively, hence all arrays have equal plan-form area.

Thumbnail sketches of each hexagonal plate in **Fig. 5** are illustrated along with their skew plate counterpart. The percentage change in perimeter length of the supporting structure with respect to the square plate datum is given adjacent to each thumbnail sketch, hence the $\pm30°$ skew plate equivalent has a 7.7% increase in perimeter length whilst the hexagonal equivalents have either a 6.5% reduction or 13.2% increase, which correspond to +30° and -30° respectively. The optimum configuration, which is not shown, corresponds to a hexagonal array with equal side lengths, whose geometric centres are arranged along a skew angle $\alpha = 26.565°$, resulting in a 6.6% reduction in perimeter length, compared with the square plate datum.

Bold lines indicate those parts of the supporting perimeter that are modelled for the 'Skew Transverse Repetition' analysis detailed in the previous section. These lines define the actual support geometry modelled for analysis, however the forty individual point constraints used to enforce these supports, giving predictions within 2% of the converged result may also be arranged as illustrated in **Fig. 4**.

Bold broken lines in **Fig. 5** are representative of those parts of the supporting perimeter that can be modelled by a conventional 'Transverse Repetition' analysis procedure. The array geometries defined by skew angles 0° and ±45° can therefore be analysed without the need for a sophisticated analysis approach because of the particular combination of aspect ration (a/b) and skew angle, leading to $\chi = 0$ in **Fig. 4**(c).

For the computer model, $\xi = 0, 0.1, ..., 0.9, 1$ in Eqn. (8), $q_{max.} = 20$ and $P = 0, 0.1, \ldots, 1.0$ in Eqn. (12).

For the composite material: $E_1 = 131.0$ kN/mm^2 (19×10^6 psi), $E_2 = 13.0$ GPa (1.89×10^6 psi), $G_{12} = 6.41$ GPa (0.93×10^6 psi) and $\nu_{12} = 0.38$. Three specially orthotropic angle ply laminates were adopted in the study. Each laminate had 20 plies with the stacking sequences defined in Table 1, which are henceforth referred to by the ESDU [25] designations S27, S32 and S41:

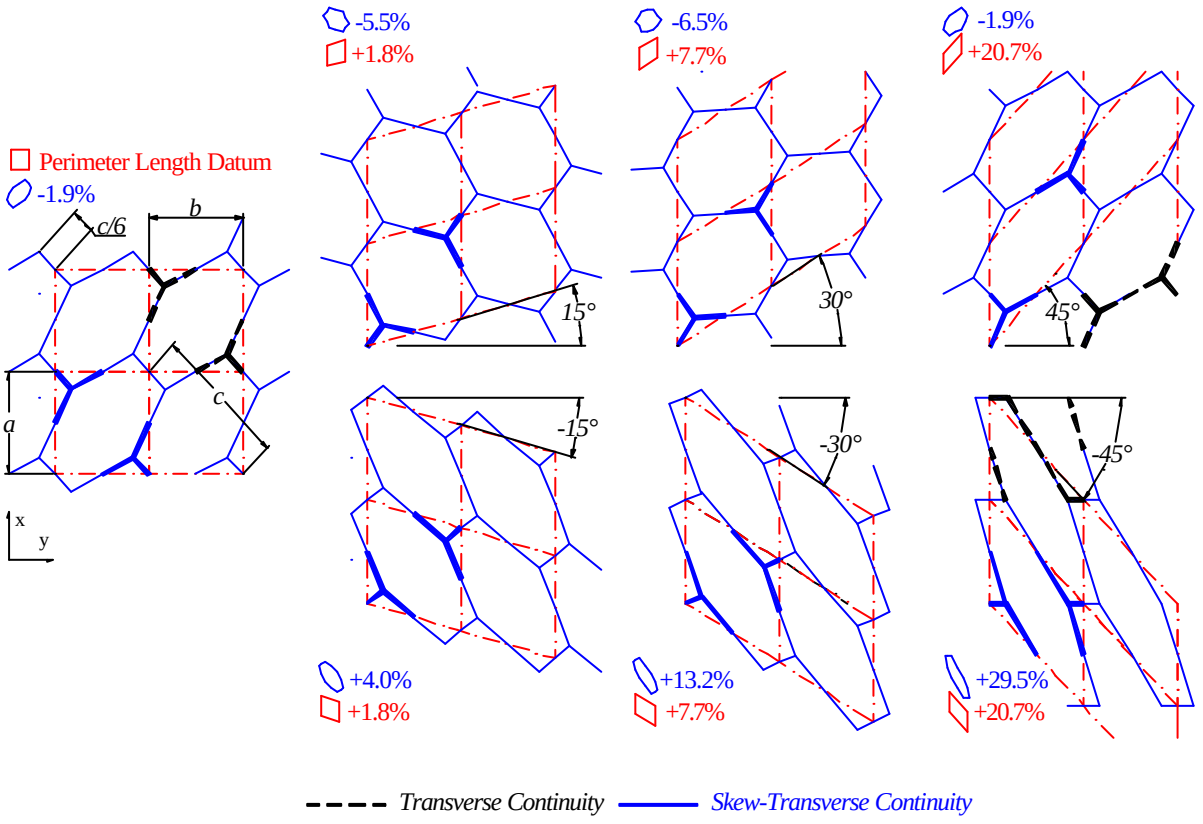

Fig. 5- The seven hexagonal planform configurations used in the study: derived through superposition, onto equal-area skew planform configurations with a = 0°, ±15°, ±30° and ±45°. Thumbnail sketches indicate the relative change in perimeter length with respect to the a = 0° datum.

Table 1 – Laminate stacking sequence definitions.

Ref.	Stacking seq.
S27	$[+q/0/-q_2/0_3/+q_2/-q]_S$
S32	$[+q/0/-q_2/0/\pm q/0_2/+q]_S$
S41	$[\pm q/0/\pm q/-q_2/0/+q_2]_S$

θ *is defined in Table 6.*

For isotropic material, E = 72.4 GPa (10.5×10^6 psi) and $\nu_{12} = 0.32$.

Plate thickness was adjusted in the isotropic case to maintain constant panel mass, based on densities of 2.8 g/cm^3 (0.1 lb/in^3) and 1.6 g/cm^3 (0.0571 lb/in^3) for aluminium and composite laminate materials respectively. This allows direct comparison of natural frequency and buckling strength for the two materials.

Results and Discussion.

Validation of the new theoretical procedure for continuous skew plates was performed by comparison with isotropic results in the literature [11]. These comparisons are given for simply supported, (bi-axial) continuous and clamped plates in **Table 2** - **Table 4**, respectively, using the dimensionless frequency factor:

$$\Omega = \omega a^2 \sqrt{(\rho h/D)} \qquad (14)$$

where ω, a, ρ, h and D are the circular natural frequency, length, density, thickness and flexural rigidity of the plate, respectively.

Table 2 – Simply support frequency factor, W

Skew Angle, α	0°	30°	45°
Ref. [12]	19.74	27.90†	43.17†
Ref. [11]	19.74	24.92	35.04

† uni-axial continuity results

Table 3 – Continuous frequency factor, W

Skew Angle, α	0°	30°	45°
Ref. [12]	19.74	29.19	47.22
Ref. [11]	19.74	29.19	47.22

Table 4 – Clamped frequency factor, W

Skew Angle, α	0°	30°	45°
Ref. [12]	35.99	46.42	66.46
Ref. [11]	35.99	46.09	65.64

Good correlation is achieved for all cases except the skewed (α = 30° and 45°) results of Table 2. This is because the current analysis assumes that panels repeat in the longitudinal direction (uni-axial continuity), hence convergence is only expected in the rectangular case, for which modes are equal or opposite in adjacent bays.

Table 5 illustrates further comparisons with results in the literature, together with ABAQUS [17] FEM results [35], for simply supported skew plates with various side length (a/b) ratios. Note that the planform area of these plates reduces with increasing skew angle, α. The bottom row (italicized) corresponds to the new uni-axial continuity results and is therefore an upper-bound on the other, simply supported, results in **Table 5**.

With the exception of the in-plane load results of **Table 7**, all other results in this paper have equal plan-form area together with a modified frequency factor, Ω', have been chosen to allow direct comparison of hexagonal, skew and square plate arrays for the composite and isotropic materials:

Table 5 – Comparison of frequency factor (Ω) results for simply support skew plates (α = 15°, 30° and 45°) with side aspect ratio *a*/*b* = 0.5, 1.0, 1.5 and 2.0.

α	15°				30°				45°			
(*a*/*b*)	0.5	1.0	1.50	2.0	0.5	1.0	1.5	2.0	0.5	1.0	1.5	2.0
Ref:												
[7]		20.87				24.91				34.79		
[30]					15.98	25.21	41.22	63.98				
[31]		20.82				25.07				34.94		
[32]	13.11	20.87		52.42	15.89	24.92		63.54	22.91	35.04		91.65
[33]						24.96				35.33		
[34]		20.92				24.97				34.64		
[35]†	12.80	20.47	33.52	51.92	15.38	24.24	40.04	62.68	21.57	33.29	55.98	89.39
[12]‡	*13.44*	*21.54*	*34.70*	*53.08*	*17.41*	*27.90*	*43.77*	*66.01*	*27.37*	*43.17*	*64.69*	*96.42*

† ABAQUS FEM [17]; ‡ Uni-axial continuity

$$\Omega' = \frac{\omega^2 a^4 \rho h}{\left(D_{11} + 2\left(D_{12} + 2D_{66}\right) + D_{22}\right)} \qquad (15)$$

$$k' = \frac{\sigma_L b^2 h}{\pi^2 \left(D_{11} + 2\left(D_{12} + 2D_{66}\right) + D_{22}\right)} \qquad (16)$$

where the D_{ij} are the flexural stiffness terms as in Eqn. (1).

Table 6 gives closed form solution results for the square and infinitely long plate using Eqns (1) and (15). A modified buckling factor:

by which the results of Eqn. (1) are non-dimensionalised, is also presented together with the buckling stress, σ_L, natural frequency, n, and the wavelength, λ, of the coincident modes of the buckling and vibration problem. The three composite angle-ply materials, S27, S32 and S41 are compared to the equivalent isotropic square plate of equal mass. They each have

Table 6 – Closed form buckling solutions and corresponding vibration results for (a) square plates (*a*/*b* = 1) and (b) infinitely long panels (*a*/*b* = ¥).

(a)

	S27			S32			S41			Iso.
θ	30	45	60	30	45	60	30	45	60	
$\sigma_{L,a/b=1}$	378.5	408.6	378.5	389.5	423.1	389.5	411.6	452.7	411.6	168.1
n	1.36	1.41	1.36	1.38	1.44	1.38	1.42	1.49	1.42	0.68
λ = 30, k' = 1.00, Ω' = 9.87										
(b)										
$\sigma_{L,a/b=\infty}$	308.3	386.4	377.1	325.3	407.8	389.5	359.0	447.5	405.4	168.1
λ	49.39	38.83	31.83	48.34	37.22	30.02	46.30	34.08	26.30	30.00
k'	0.81	0.95	1.00	0.84	0.96	1.00	0.87	0.99	0.99	1.00
n	0.74	1.06	1.28	0.78	1.14	1.38	0.86	1.30	1.42	0.68
Ω'	5.41	7.41	9.28	5.60	7.81	9.86	5.97	8.64	11.17	9.87

three variants corresponding to the angle ply, θ, direction given in **Table 1**, i.e. θ = 30°, 45° and 60°. For the square plate case of **Table 6**(a), the buckling stress, σ_L, and natural frequency, n, vary significantly between the three composite materials, coupled with changes in angle ply direction, θ, by up to 19.6% and 9.4% respectively. Note that λ = 30, k' = 1.00, Ω' = 9.87 is shared by all of these results. Comparing equal mass isotropic and composite materials reveals that the composite material has increases of up to a 169.3% and 117.4% in σ_L and n above the isotropic material, respectively. For the infinitely long plate of **Table 6**(b), these results change to 45.1% and 90.2% for the composite cases and 166.2% and 107.3% when comparing the isotropic and composite material respectively. The ratio of the maximum buckling stresses, σ_L, in the composite and isotropic materials is 2.69 and 2.66 and for natural frequency, n, 2.17 and 2.07 respectively. The dimensionless parameters, however, fail to demonstrate these relative differences.

The design curves of **Fig. 6** demonstrate the relationship between the modified frequency factor Ω' of Eqn. (15) and skew angle, α. The three laminates S27(θ), S32(θ) and S41(θ) of **Table 1** are shown for the angle ply directions θ = 30, 45 and 60°.

For the positive skew angles on **Fig. 6**, the 30° angle ply configuration, S32(30), is seen to produce higher frequency factor results, which is probably due to the fact that the 30° direction tends to be aligned with the longest span direction of the cells, thus increasing the flexural stiffness. The quasi-isotropic laminates have this effect for configurations in which the spans directions within each cell are approximately equal.

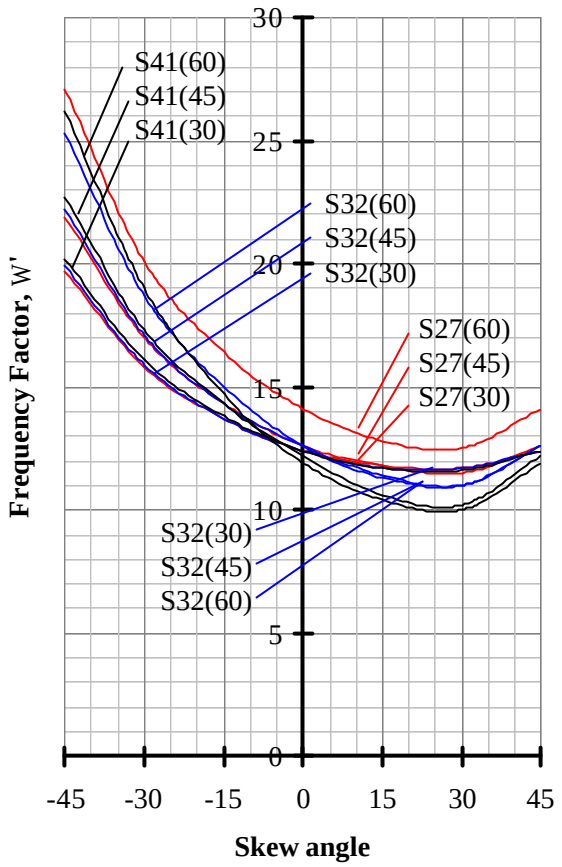

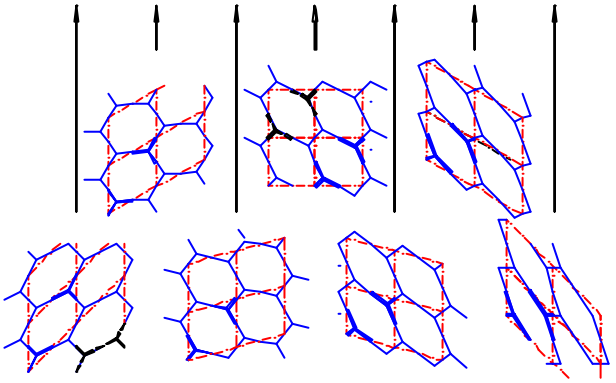

Fig. 6 – Frequency factor curves for composite hexagonal arrays of Table 1. The skew angle, a (= 0, ±15, ±30 and ±45), defines the hexagonal planform shape, illustrated below the figure, cf. Fig. 5.

The final set of results presented in this paper relate to the effect of in-plane compressive stress on continuous skew plate arrays. The results are presented in **Table 7** for the same set

of skew angles and aspect ratios as in **Table 5**. The results complement those of **Table 5** by allowing comparisons to be made between isolated, uni-axial and bi-axial continuity. Note that changes in skew angle result in a change in planform area for these three sets of results. The ratio of applied stress to the buckling stress, $\sigma_L/\sigma_{L,critical}$, given in **Table 7** varies with plate aspect ratio and has therefore been calculated against published results [15]. Frequency factor, Ω (see Eqn (14)), results are given for the unloaded case, $\sigma_L/\sigma_{L,critical} = 0$, followed by the percentage reduction in Ω with increasing in-plane compressive stress $\sigma_L/\sigma_{L,critical} = 0.5$, 0.8 and 0.95.

Table 7 – Skew plate array frequency factors, W, for a = (a) 15°, (b) 30° and (c) 45°, with percentage reduction due to in-plane compressive stress.

(a) a **= 15°**

a/*b*	$\sigma_L/\sigma_{L,critical}$.			
	0	0.5	0.8	0.95
0.5	13.49	-29%	-55%	-78%
1	21.82	-29%	-55%	-78%
1.5	35.30	-26%	-49%	-64%
2	53.96	-18%	-31%	-38%
2.5	77.84	-13%	-23%	-52%

(b) a **= 30°**

a/*b*	$\sigma_L/\sigma_{L,critical}$.			
	0	0.5	0.8	0.95
0.5	17.64	-29%	-55%	-78%
1	29.19	-29%	-55%	-78%
1.5	46.81	-23%	-40%	-51%
2	70.55	-15%	-26%	-32%
2.5	100.60	-11%	-18%	-22%

(c) a **= 45°**

a/*b*	$\sigma_L/\sigma_{L,critical}$.			
	0	0.5	0.8	0.95
0.5	28.07	-29%	-54%	-75%
1	47.23	-21%	-39%	-56%
1.5	75.41	-13%	-21%	-26%
2	112.29	-8%	-14%	-17%
2.5	158.14	-6%	-10%	-12%

Concluding remarks

A new theoretical approach to the assessment of natural frequency response of rigid, cellular supported plate arrays has been presented. Excellent agreement has been demonstrated with the limited results available in the literature for skew plate arrays. The study has also demonstrated the implications of composite tailoring on the frequency response of plate arrays when coupled with complex geometrical arrangements of rigid supports. Finally, a quantitative assessment of the effects of in-plane (static) compressive stress has been shown for a range of skew plate array configurations.

References and Bibliography

[1] Timoshenko, S. *Vibration problems in engineering*. 3rd edition, D. Van Nostrand Company Inc., 1955.

[2] Meirovitch, L. *Analytical methods in vibrations*. Macmillan series in applied mechanics, The Macmillan Company, 1967.

[3] Chen, Y. *Vibration: Theoretical methods*, Addison-Wesley Publishing Company Inc., 1966.

[4] Bardell, N.S. The free vibration of skew plates using the Hierarchical Finite Element Method. *Computers and Structures*, Vol. 45, No. 5/6, pp. 841-874, 1992.

[5] Mizusawa, T., Kajita, T. and Naruoka, M. Analysis of skew plate problems with various constraints. *Journal of Sound & Vibration*, Vol. 73, No. 4, pp. 575-584, 1980.

[6] Dawe, D. J. and Peshkam, V. Buckling and vibration of finite length composite prismatic plate structures with diaphragm ends, Part 1: Finite strip formulation. *Computer Methods in Applied Mechanics and Engineering*, Vol. 77, pp. 1-30, 1989.

[7] Nair, P. S. and Durvasula, S. Vibration of skew plates. *Journal of Sound & Vibration*, Vol. 26, No. 1, pp. 1-19, 1973.

[8] Roberts, S. B. Buckling and vibration of polygonal and rhombic plates. *Proc. ASCE EM* Vol. 97, No. 2, pp 305-15, 1971.

[9] Laura, P.A.A and Rossi, R.E. Letters to the editor: Transverse vibrations of a thin, elastic plate of regular hexagonal shape. *Journal of Sound & Vibration*, Vol. 256, No. 2, pp. 367-372, 2002.

[10] Mizusawa, T. and Kajita, T. Vibration of continuous skew plates. *Earthquake Engineering and Structural Dynamics*, Vol. 12, pp 847-850, 1980.

[11] Bardell, N. S. and Langley, R. S. Some Observation on the form of the phase constant surface of a periodic skew plate. *Proc 5th International Conference on Recent Advances in Structural Dynamics*, University of Southampton, 18-21 July, 1994.

[12] York, C. B. and Yusuf, S. R. *Vibration theory and results for infinitely wide skew plates*. University of Glasgow, Department of Aerospace Engineering Research Report, 04-02, 2004.

[13] York, C. B. and Williams, F. W. Theory and buckling results for infinitely wide stiffened skew plate assemblies. *Composite Structures*, Vol. 28, pp. 189-200, 1994.

[14] York, C. B. Elastic buckling design curves for isotropic rectangular plates with continuity or elastic edge restraint against rotation. *Aeronaut. J.*, Vol. 104 No. 1034, pp. 175-182, 2000.

[15] York, C. B. Influence of continuity and aspect ratio on the buckling of skew plates and plate assemblies. *International Journal of Solids Structures*, Vol. 33, No. 15, pp. 2133-2159, 1996.

[16] York, C. B. Buckling interaction in regular arrays of distorted hexagonal plates. *Aeronaut. J.*, Vol. 107, No. 1074, pp. 461-468, 2003.

[17] ABAQUS/Standard, Version 5.8, Hibbit, Karlsson and Sorensen, Inc., 1998.

[18] Lurie, H. Lateral vibrations as related to structural stability, *Journal of Applied Mechanics*, Vol. 74, pp. 195-204, 1952.

[19] Wittrick, W. H. and Williams, F. W. Buckling and vibration of anisotropic or isotropic plate assemblies under combined loadings. *Int. J. Mech. Sci.*, Vol. 16, pp. 209-239, 1974.

[20] Wittrick, W. H. and Williams, F.W. A general algorithm for computing natural frequencies of elastic structures. *Quart. J. Mech. Appl. Math.*, Vol. 24, pp. 263-284, 1971.

[21] Williams, F. W. and Anderson, M. S. Buckling and vibration analysis of shear-loaded prismatic plate assemblies with supporting structures, utilizing symmetric or repetitive cross-sections. In *Aspects of the analysis of plate structures - a volume in honour of W. H. Wittrick* (ed. Dawe, D. J., Horsington, R. W., Kamtekar, A. G. and Little, G. H.), Oxford University Press, Oxford, pp. 51-71, 1985.

[22] York, C. B. and Yusuf, S. R. *Vibration response of skew plates with in-plane loading, below initial buckling*. University of Glasgow, Department of Aerospace Engineering Research Report, 04-03, 2004.

[23] York, C. B. and Yusuf, S. R. *Natural frequency response of rigid cellular supported composite face sheets*. University of Glasgow, Department of Aerospace Engineering Research Report, 04-04, 2004.

[24] Liew, K. M. and Wang, C. M. Flexural vibration of in-plane loaded plates with straight line/curved internal supports. *Journal of Vibration and Acoustics, ASME*, Vol. 115, pp. 441-7, 1993.

[25] Engineeering Sciences Data Unit, *Laminate stacking sequences for special orthotropy*. ESDU 82013, 1982.

[26] York, C. B. Elastic buckling interaction in regular arrays of distorted composite hexagonal plates. *Proc. American Helicopter Society Hampton Roads Chapter, Structure Specialists' Meeting*, Williamsburg, VA, 2001.

[27] Engineering Sciences Data Unit, *Natural frequencies of rectangular, special orthotropic laminated plates*. ESDU 83036, 1983.

[28] Engineering Sciences Data Unit, *Natural frequencies of rectangular flat plates with various edge conditions*. ESDU 75030, 1975.

[29] Engineering Sciences Data Unit, *Natural frequencies of isotropic and orthotropic rectangular plates under static in-plane loading (including shear loading)*. ESDU 90016, 1990.

[30] Mizusawa, T. and Kajita, T. Vibration and buckling of skew plates with edges elastically restrained against rotation, *Computers and Structures*. Vol. 22, No. 6, pp. 987-994, 1986.

[31] Liew, K. M. and Lam, K. Y. Application of two-dimensional orthogonal plate function to flexural vibration of skew plates, *Journal of Sound and Vibration*. Vol. 139, No. 2, pp. 241-252, 1990.

[32] Bardell, N. S. The Free vibration of skew plates using the Hierarchical Finite Element Method, *Computers and Structures*. Vol. 45, No. 5/6, pp. 841-874, 1992.

[33] Wang, S. Vibration of thin skew fibre reinforced composite laminates, *Journal of Sound and Vibration*. Vol. 201, No. 3, pp. 335-352, 1997.

[34] Reddy, A. R. K. and Palaninathan, R. Free vibration of skew laminates, *Computers and Structures*. Vol. 70, No. 4, pp. 415-23, 1999.

[35] York, C. B. and Yusuf, S. R. *Natural frequencies of undamped vibrations in skew plates with edge restraint against rotation*. University of Glasgow, Department of Aerospace Engineering Research Report, 04-05, 2004.